

A Discussion
on
Impulse Breakdown and Discharge Propagation Mechanisms in Air

by

NIRMALYA BASU

Date of Birth: May 3, 1984

Qualification: Master of Engineering in Electronics and Telecommunication Engineering

Email: nirmalya1basu@gmail.com, nirmalya_bs@yahoo.co.in

Mobile: +919007757186

Contents

	<i>Page</i>
1. Introduction	1
2. Method	1
3. Details	2
<i>3.1. Breakdown mechanism at $g = 15$ mm.</i>	<i>2</i>
<i>3.2. Breakdown mechanism at $g = 100$ mm.</i>	<i>4</i>
<i>3.3. Influence of Gap Distance on Breakdown Mechanism</i>	<i>6</i>
<i>3.4. Breakdown Mechanism in the Transition Region</i>	<i>7</i>
<i>3.5. Observations on Breakdown and Discharge Propagation Mechanisms</i>	<i>10</i>
4. Conclusion	12
References	14

1. Introduction

The authors in [1] have described an experimental study which they carried out for gaining clarity on the mechanism of impulse breakdown of air under non-uniform electric field.

It has been observed that in gap discharge in air under non-uniform electric field, a secondary streamer initiates after the primary streamer has reached the grounded electrode. The mechanism is generally conceived as follows. At first, the primary streamer creates a channel through which the secondary streamer propagates and in the process, heats it up, thereby leading to a breakdown. However, it was felt by the authors that further clarity was necessary on the discharge propagation mechanism, and it is to achieve this, that the present study has been carried out. The focus has been on the process of discharge propagation from streamer initiation to breakdown. The authors have also discussed the key mechanism that determines breakdown in air.

2. Method

The experimental setup is shown in the following figure (fig. 1).

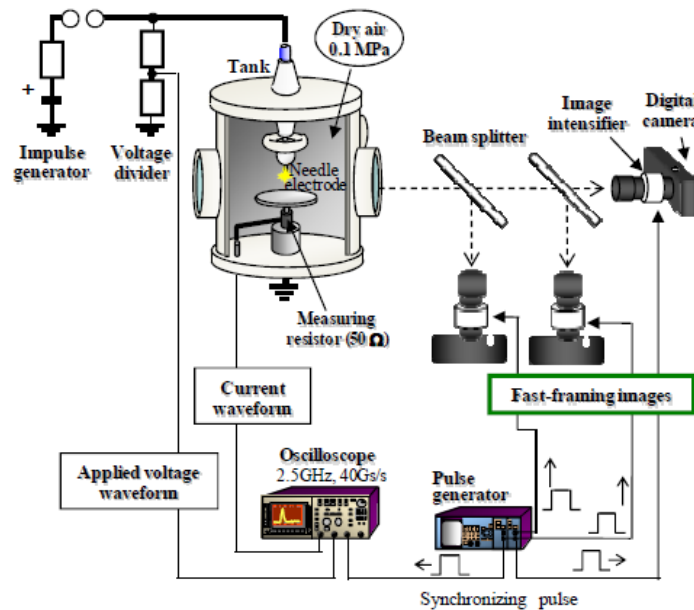


Fig. 1. Experimental Setup (reproduced from [1])

A needle electrode and a plane electrode are kept in a tank filled with dry air at 0.1 MPa as shown in the above figure. The electrodes are made of stainless steel. The length of the needle is 20 mm. and its tip diameter is 1 mm. A positive lightning impulse voltage ($1.2 / 50 \mu\text{s}$) has been applied to generate the discharge between the two electrodes. A 50Ω measuring resistor has

been used to measure the discharge current. A photomultiplier tube has been used to obtain the light intensity waveform. Fast framing images of the discharge have been obtained using 3 digital cameras with image intensifiers by successively exposing them. Their exposure times have been controlled in the order of nanoseconds. The discharge current and light intensity waveforms and the fast-framing images could be synchronously obtained in 20-200 ns by using a pulse generator. Observations are made by varying the gap distance (g) from 15 mm. to 100 mm.

3. Details

Two types of breakdown mechanism from streamer initiation to breakdown have been found to exist. This has been presented by the authors in [2]. In [2], observations for two distinct cases have been presented— one, for $g = 15$ mm. and another, for $g = 100$ mm.

3.1 Breakdown mechanism at $g = 15$ mm.

The following figure (fig. 2) shows the discharge current and fast-framing images at $g = 15$ mm. under the application of breakdown voltage (29 kV).

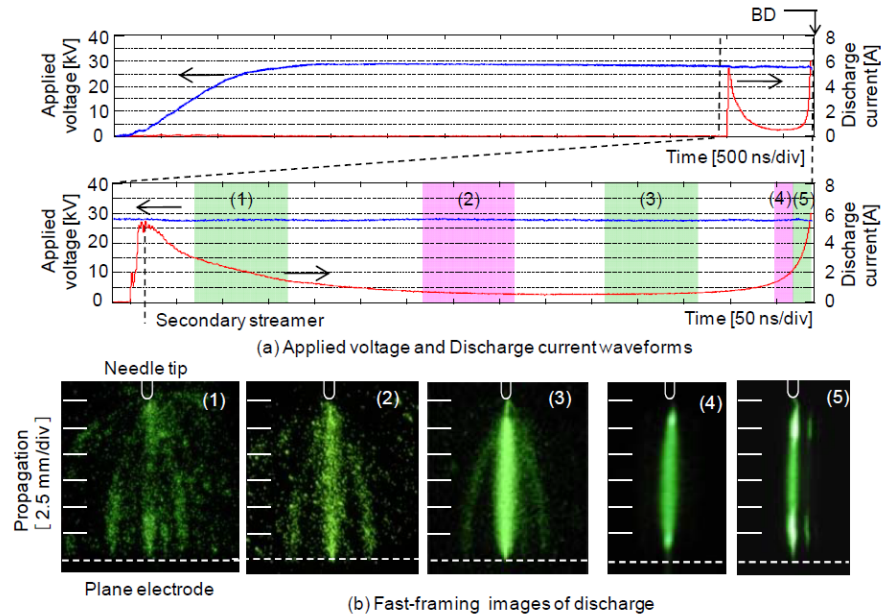


Fig. 2. Discharge Current Waveform and Fast-framing Images Leading to Breakdown ($g = 15$ mm., $V_a = 29$ kV) (reproduced from [2])

As can be observed from fig. 2, the discharge current reaches a peak (due to initiation of the secondary streamer), then reduces rapidly to almost zero and after about 800 ns, the discharge current rises again and breakdown occurs. As is evident from fig. 2 (b) (1) and (2), a number of

secondary streamers first arrive at the plane electrode after arrival of the primary streamer at this electrode [3] and as a result, the conductive paths are formed. Then, the shortest conductive path brightens up (as shown in fig. 2 (b) (3)) because the temperature of this plasma channel rises due to Joule heating as discharge current flows through it. This raises the conductivity of this channel. The other channels gradually disappear. This happens because the rise in conductivity of the shortest channel results in the discharge current concentrating in this path. After that, breakdown initiates from both the needle as well as the plane electrodes as shown in fig. 2 (b) (4) and (5). From this, it is evident that the current concentrates on the hot spots of the two electrodes when the channel is heated.

The breakdown mechanism for this case is considered to be as follows [3]. The electrical conducting path bridging the two electrodes forms when the secondary streamers reach the plane electrode. But this does not immediately lead to breakdown. This is because the conductivity of the channel is not high enough. When the electrons injected from the plane electrode move into the channel, the electrons obtain energy from the applied electric field and give the energy to the channel, which increases the temperature and the conductivity of the channel. Breakdown occurs when the conductivity of the channel becomes high enough.

It is worthwhile mentioning here that the initiation of the primary and the secondary streamers have been distinctly observed, as presented in [3]. Under similar conditions, the following waveforms have been obtained.

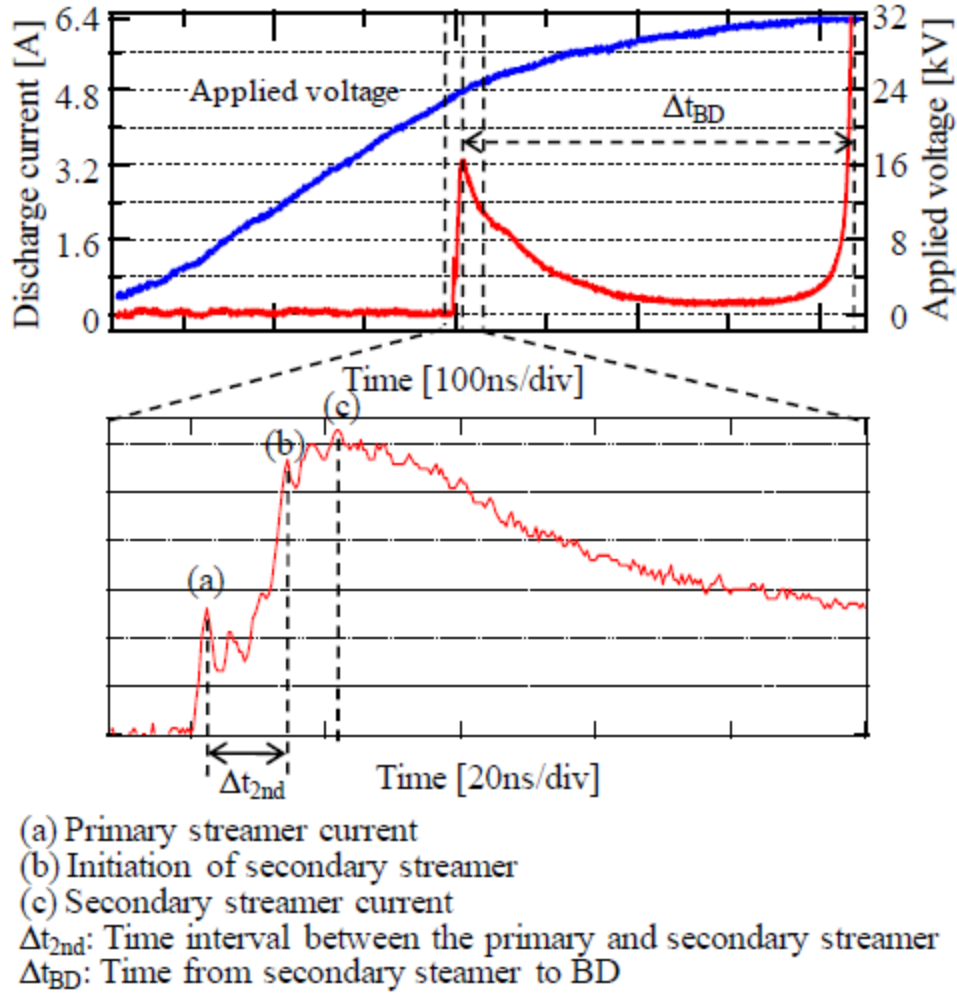


Fig. 3. Definition of primary and secondary streamer current and time to BD (reproduced from [3])

As shown here (fig. 3), the peak (a) in the discharge current waveform denotes the primary streamer current and the peak (b) denotes the inception of the secondary streamer.

3.2 Breakdown mechanism at $g = 100 \text{ mm}$.

Breakdown occurs in quite a different manner when the electrodes are kept at distance of 100 mm. from each other. This is evident from the waveforms and the images presented in the following figure (fig. 4).

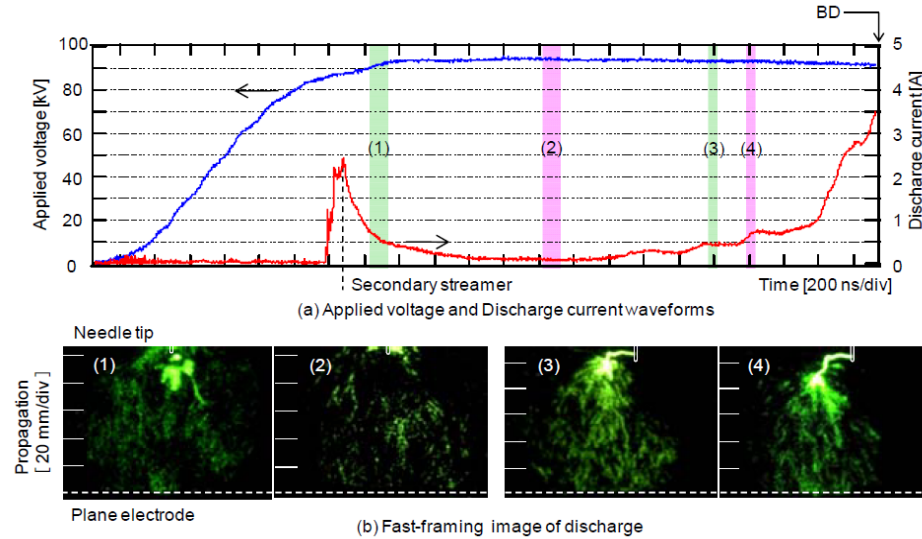


Fig. 4. Discharge Current Waveform and Fast-framing Images Leading to Breakdown ($g = 100$ mm., $V_a = 94$ kV) (reproduced from [2])

As shown in fig. 4 (a), the discharge current decreases after propagation of the secondary streamer. But after about $1.5 \mu\text{s}$, it rises again and finally, breakdown occurs. Interestingly, in this case, when the discharge current rises again before breakdown, it does so step by step. The intense light that is emitted and propagated from the needle electrode (shown in fig. 4 (b) (1)) is due to the secondary streamer. But, it does not reach the grounded plane electrode due to the long gap length. Hence, as fig. 4 (b) (2) depicts, no high conductive channel bridging the two electrodes is formed. However, the leader channel propagates from the needle electrode as shown in fig. 4 (b) (3) and (4). But, it initiates not from the tip, but from the side of the needle. This behavior of the leader can be interpreted in terms of the space charge behavior [4] as shown schematically in fig. 5 below.

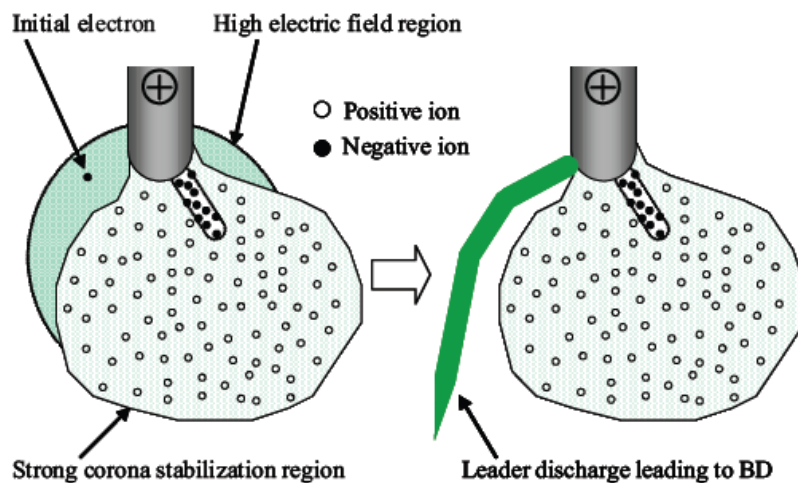


Fig. 5. Schematic Illustration of Leader Discharge Propagation Leading to Breakdown (reproduced from [4])

Many residual positive ions are left in the space beneath the needle. They tend to reduce the electric field strength in the vicinity of the needle tip. However, the adjacent space designated by hatched area in fig. 5 has relatively high electric field strength. When an electron appears in this space, a leader discharge starts to propagate. Thus, the leader discharge is obliged to propagate along the periphery of the positive charge space in the vicinity of the needle electrode.

Breakdown occurs when the leader discharge reaches the grounded plane electrode leading to the formation of a high conductive channel in the gap. Several streamers propagate from the leader head and they bridge the gap between the electrodes. One of them gets selected and it gets turned to the leader channel. The discharge current rises with repeating step-like increase. The discharge current does not become zero after it rises again. This makes it evident that the leader channel bridges the gap constantly; but the light emitted from the streamer region is less intense than that from the leader region since the conductivity of the streamer is low.

3.3 Influence of Gap Distance on Breakdown Mechanism

In [2], the authors have also stated that the mechanism of breakdown changes as shown in the following figure (fig. 6).

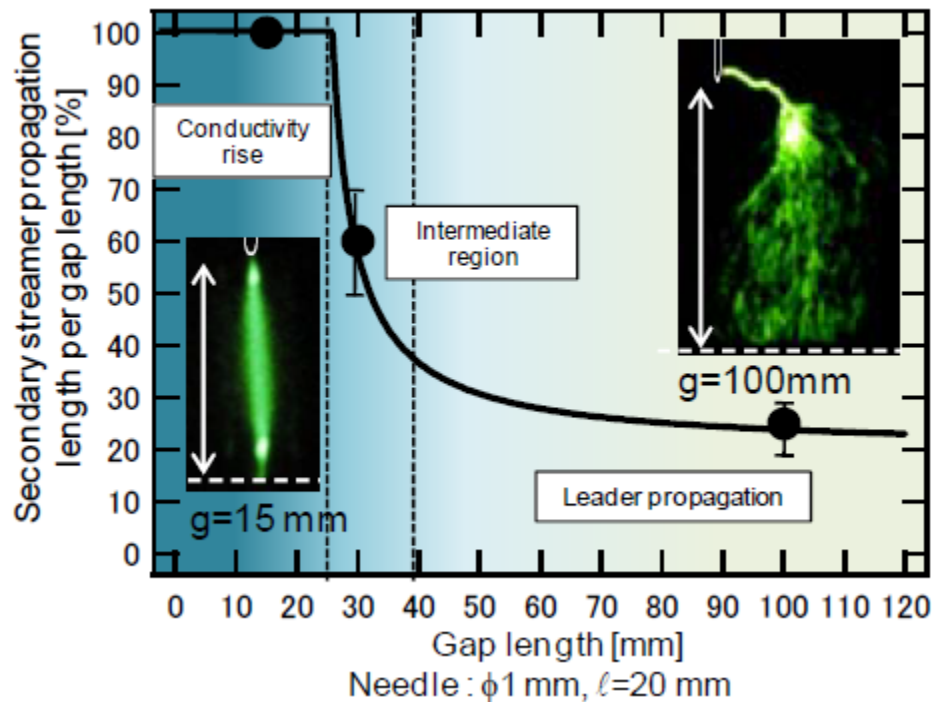


Fig. 6. Influence of Discharge Propagation Mechanism on Gap Length (reproduced from [2])

From fig. 6, it is evident that for $g < 30$ mm., breakdown occurs by rise of the conductivity of the secondary streamer, but for $g > 30$ mm., breakdown is caused by propagation of the leader. The above discussions imply that the breakdown mechanism is primarily dependent on the behavior of the secondary streamer.

3.4 Breakdown Mechanism in the Transition Region

The mechanism of breakdown occurring in the intermediate or the transition region (shown in fig. 6) has been investigated in [1].

The following figure (fig. 7) depicts the observations made on the progress of discharge leading to breakdown when breakdown voltage (i.e., 53 kV) is applied.

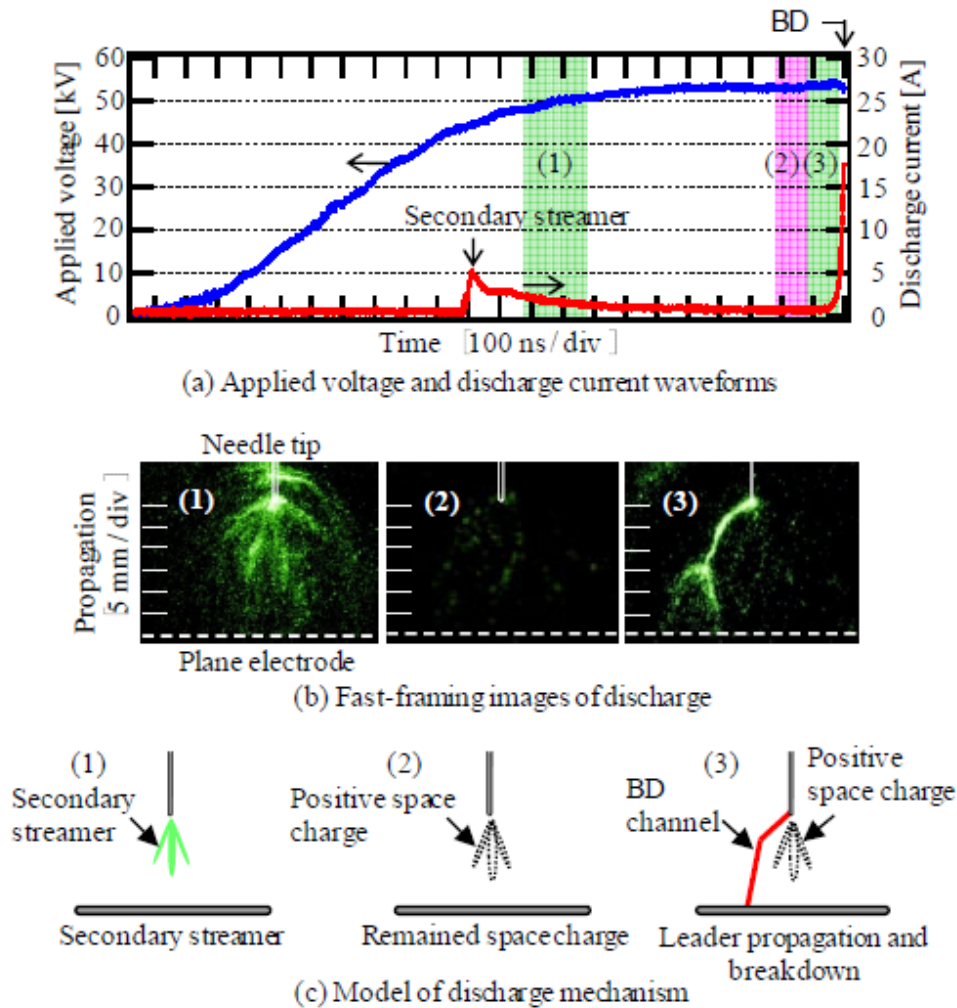


Fig. 7. Discharge current waveforms and fast-framing images leading to BD with model of BD by leader progress ($V_a = 53$ kV = BDV, $g = 30$ mm) (reproduced from [1])

As can be observed from the above figure (fig. 7), after the discharge current has reached a peak, it decreases to almost zero. However, after $1.1 \mu\text{s}$, it rises again and finally, breakdown occurs. The fast-framing images that have been taken at different instants, designated in fig. 7 (a) as (1)-(3), are reproduced from [1] in fig. 7 (b). The discharge propagation mechanism in this case is by leader propagation and is exactly similar to what happens at $g = 100 \text{ mm}$. on application of breakdown voltage (which has been described above). The model of this discharge mechanism is given in fig. 7 (c).

The observations that have been made by application of over-voltage (120% BDV, i.e., 63 kV) at $g = 30 \text{ mm}$. are given in figure 8 below.

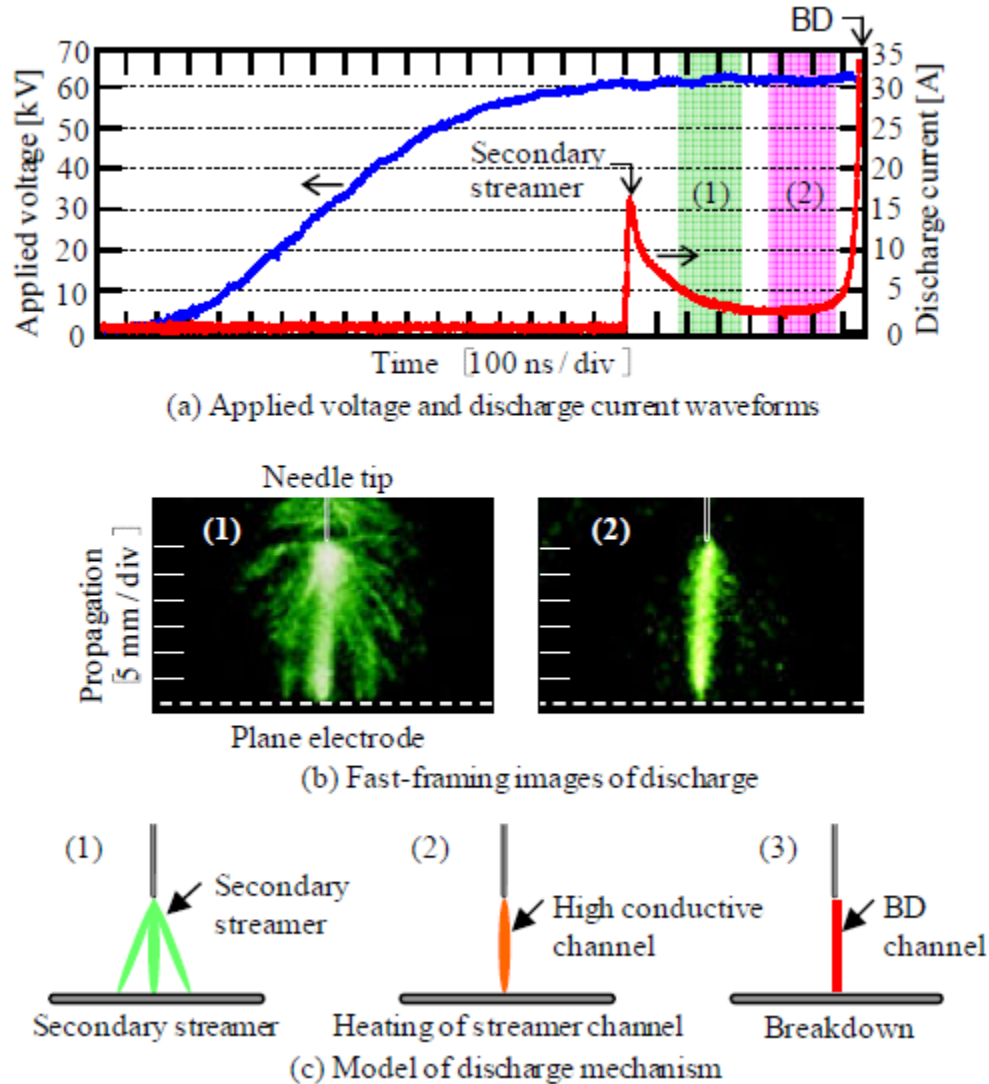
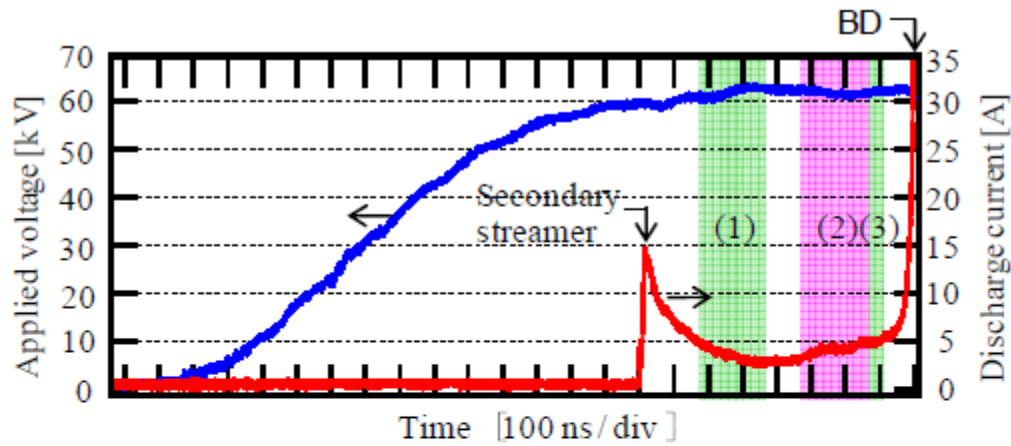


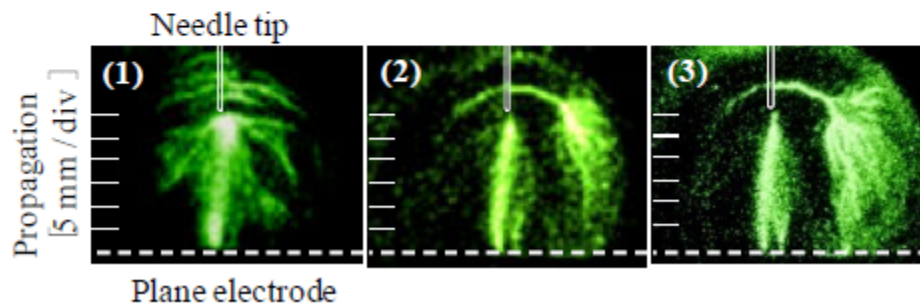
Fig. 8. Discharge current waveforms and fast-framing images leading to BD with model of BD by secondary streamer progress ($V_a = 63 \text{ kV} = 1.19 \times \text{BDV}$, $g = 30 \text{ mm}$) (reproduced from [1])

As can be observed from fig. 8 (a), the discharge current reduces after propagation of the secondary streamer (marked by occurrence the first visible peak in the current waveform given in the figure). However, after about 200 ns, the discharge current starts increasing again and eventually, breakdown takes place. Since, in this case, the applied voltage is considerably higher than that in the breakdown voltage case, the secondary streamers arising from the needle electrode can reach the grounded plate. Hence, breakdown occurs by heating and subsequent rise in conductivity of the streamer channel in a manner which is exactly similar to what happens on application of breakdown voltage at $g = 15$ mm. The model of this discharge mechanism is given in fig. 8 (c).

In the conditions similar to those of fig. 8, both types of discharge were observed at the same time as shown in fig. 9 below.



(a) Applied voltage and discharge current waveforms



(b) Fast-framing images of discharge

Fig. 9. Discharge current waveforms and fast-framing images leading to breakdown ($V_a = 64$ kV = $1.2 \times$ BDV, $g = 30$ mm.) (reproduced from [1])

In this case, as shown in fig. 9 (b) (1), the secondary streamer reaches the grounded plane electrode. This leads to formation of a highly conductive channel between the two electrodes. However, the leader channel also propagates from the needle as shown in fig. 9 (b) (2). From these results, it may be inferred that even if the secondary streamer succeeds in reaching the grounded plane electrode, it needs a few hundred nanoseconds the conductivity of the secondary streamer channel sufficiently to give rise to breakdown. In such a case, both the secondary streamer channel as well as the leader channel has a possibility of leading to breakdown.

3.5 Observations on Breakdown and Discharge Propagation Mechanisms

The following figure (fig. 10) depicts how propagation of the secondary streamer and the discharge mechanism vary with the gap distance.

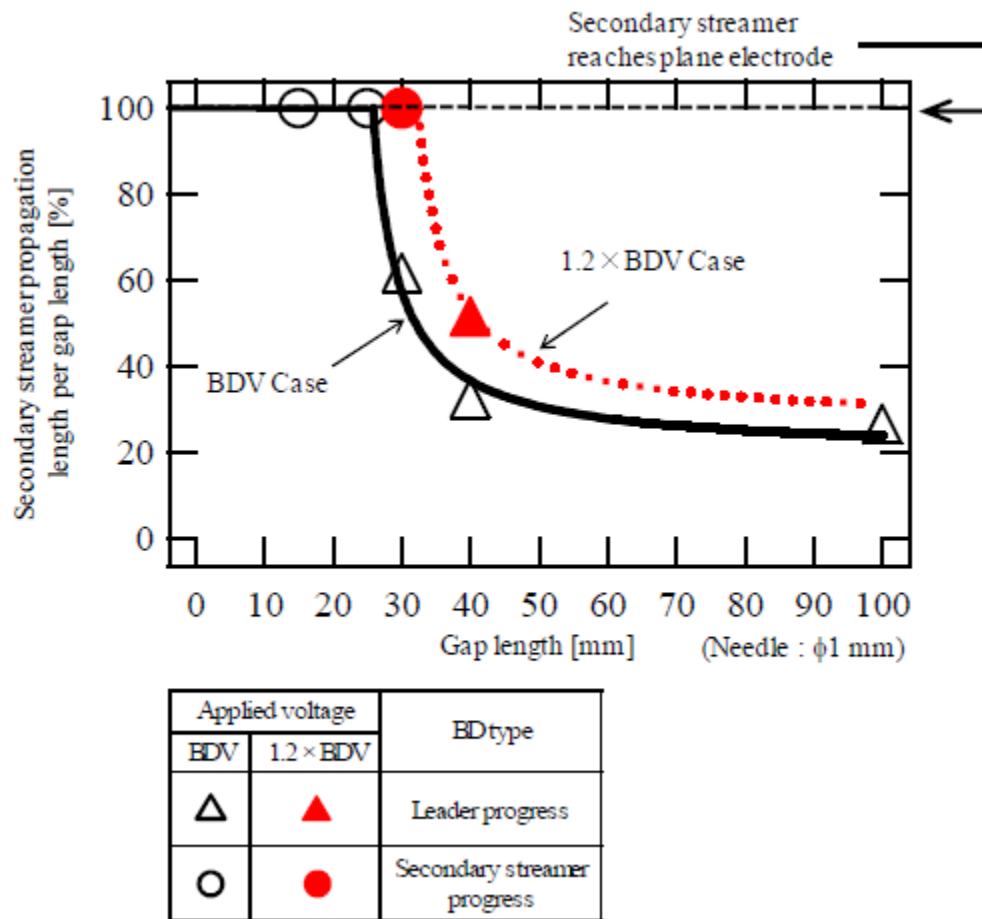


Fig. 10. Discharge propagation mechanisms shown in the graph of secondary streamer propagation length per gap length vs. gap length (reproduced from [1])

We observe that in the breakdown voltage case, the larger the gap length is, the smaller is the proportion of progress of the secondary streamer. Moreover, at each gap length, the proportion of secondary streamer progress is larger in the overvoltage case than that in the breakdown voltage case. In this case, application of overvoltage leads to change of breakdown mechanism from leader progress to secondary streamer progress at a gap length of around 30 mm. From these results, it may be inferred that the proportion of progress of the secondary streamer is greater if the gap distance is lower and the applied voltage is higher.

As mentioned above, even if the secondary streamer reaches the grounded plane electrode, breakdown may occur by leader progress as well. This is because the breakdown mechanism is determined by two things– (a) whether the secondary streamer can reach the grounded plane electrode or not, and (b) Joule heating and conductivity rise of the secondary streamer channel. Assuming the conductivity of the secondary streamer channel to be uniformly distributed, the Joule heat per unit length (Q) in the streamer channel can be expressed as follows:-

$$Q = \sigma S \frac{V^2}{g^2} \quad (1),$$

where σ is the conductivity of the streamer channel, V is the applied voltage, S is the cross-section of the streamer channel, i.e., the gap length. This equation implies that the Joule heat per unit length is a function of the applied voltage per gap length. Hence, when the gap is short and the applied voltage is high, Joule heat is high and therefore, the conductivity rises easily.

The following figure (fig. 11) depicts the dependence of discharge propagation mechanism on the applied voltage per unit gap length for $g = 30$ mm.

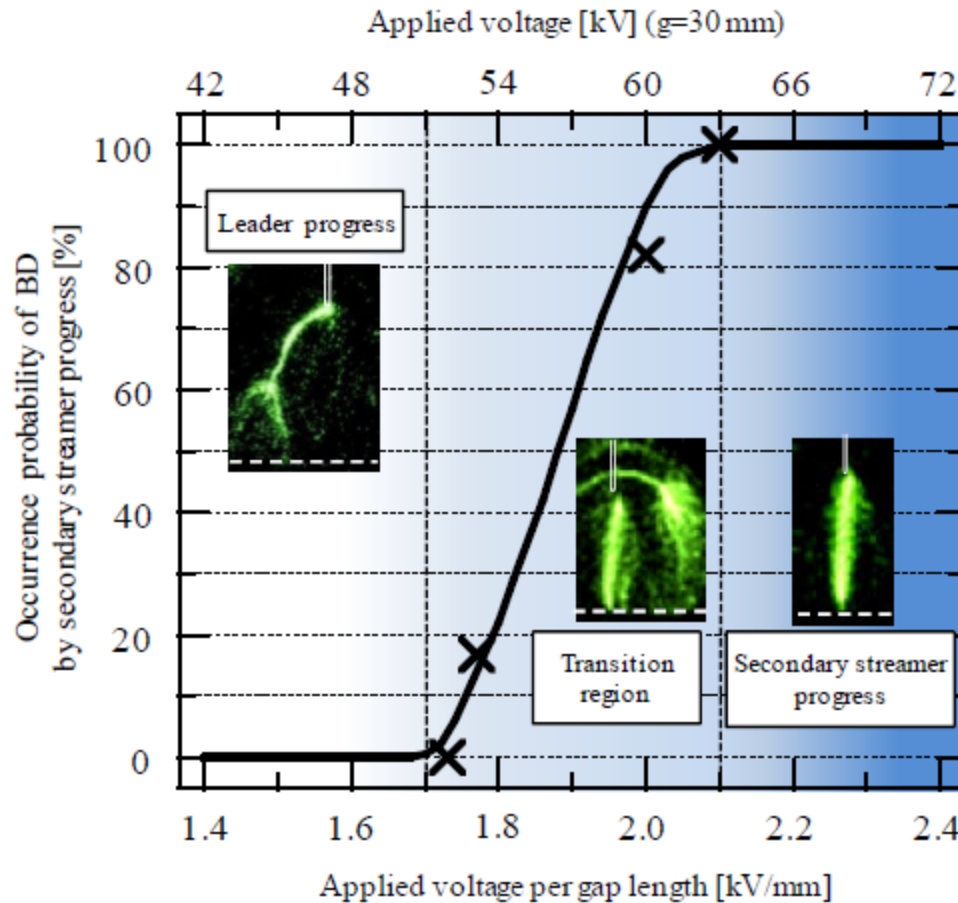


Fig. 11. Transition of discharge propagation mechanism as a function of applied voltage normalized by gap length ($g = 30$ mm) (reproduced from [1])

In the region of lower applied voltage, all breakdowns occur as a result of leader progress. With increase in the applied voltage, the probability of breakdown by secondary streamer progress increases rapidly. This is because increase in the applied voltage leads to increased Joule heating. These results suggest that in case of breakdown by secondary streamer progress, the discharge propagation mechanism is governed by Joule heating and by the resultant conductivity rise of the streamer channel arriving at the grounded plane electrode.

4. Conclusion

In the above, the mechanisms of impulse breakdown of an air-gap have been discussed. The focus has been on the formation of the discharge channel. The study has led to the following inferences:-

1. Two breakdown mechanisms have been observed – one, due to leader progress and another, due to secondary streamer progress.

2. The breakdown mechanism depends on the gap length and based on a study of this dependence, a transition region has been arrived at. In this case, it has been found to be at around $g = 30$ mm.
3. For each gap length, the proportion of the secondary streamer progress at over-voltage is larger than that at the breakdown voltage. This leads to the conclusion that the breakdown mechanism is dependent on the applied voltage per gap length.
4. The arrival of the secondary streamer at the grounded electrode is one of the key factors determining the breakdown mechanism.
5. Another key factor determining the breakdown mechanism is the Joule heating of the secondary streamer channel. Its role is observable in the transition region. This has been found to depend on the applied voltage per gap length.

References

1. K. Hotta, T. Iwata, H. Kojima, N. Hayakawa, N. Yanagita, T. Kato, T. Rokunohe and H. Okubo, "Impulse Breakdown Mechanism Based on Discharge Propagation Process under Non-uniform Electric Field in Air", IEEE Conference on Electrical Insulation and Dielectric Phenomena, October 2011, pp. 534-537.
2. H. Kojima, K. Hotta, T. Iwata, N. Hayakawa, N. Yanagita, T. Kato, T. Rokunohe and H. Okubo, "Influence of Gap Length on Discharge Channel Propagation and Breakdown Mechanism in Air", XVII International Symposium on High Voltage Engineering, August 2011.
3. T. Iwata, H. Kojima, N. Hayakawa, F. Endo, N. Yanagita, T. Kato, T. Rokunohe, and H. Okubo, "Positive Streamer Propagation and Breakdown Characteristics in Non-uniform Air Gap," 2nd ICHVE, pp. 377-380, 2010.
4. N. Hayakawa, K. Hotta, S. Okabe, and H. Okubo, "Streamer and Leader Discharge Propagation Characteristics Leading to Breakdown in Electronegative Gases," IEEE Trans. Dielectr. Electr. Insul. vol.13, No. 4, pp. 842-849, 2006.